



A highly selective and sensitive probe based on benzo[1,2-b:4,5-b']dithiophene: synthesis, detection for Cu(II) and self-assembly



Yuwen Ma^a, Taohua Leng^b, Guoqiao Lai^c, Zhifang Li^c, Xiaojia Xu^a, Jianwei Zou^{d,*},
Yongjia Shen^a, Chengyun Wang^{a,*}

^a Key Laboratory for Advanced Materials and Institute of Fine Chemicals, East China University of Science & Technology, Shanghai 200237, PR China

^b National Food Quality Supervision and Inspection Center (Shanghai)/Shanghai Institute of Quality Inspection and Technical Research, Shanghai 200233, PR China

^c Key Laboratory of Organosilicon Chemistry and Material Technology of Ministry of Education, Hangzhou Normal University, Hangzhou 310012, PR China

^d Ningbo Institute of Technology, Zhejiang University, Ningbo 315100, PR China

ARTICLE INFO

Article history:

Received 8 January 2016

Received in revised form 3 March 2016

Accepted 8 March 2016

Available online 10 March 2016

Keywords:

Fluorescent dyes

Benzo[1,2-b:4,5-b']dithiophene

Picolinamide

Turn-off probe

Self-assembly

ABSTRACT

A novel turn-off probe for copper(II) containing benzo[1,2-b:4,5-b']dithiophene (BDT) and two picolinamide units was synthesized. In this probe, two picolinamide units complex with one Cu²⁺ ion and two nitrogen atoms in each picolinamide unit coordinate with Cu²⁺, which is verified by DFT calculation. Its fluorescence quantum yield is 0.43 and the detection limit is as low as 2.4 × 10⁻⁸ mol/L. The results show that the probe displays good selectivity for Cu²⁺ over other ions (Mn²⁺, Pb²⁺, Cr³⁺, Zn²⁺, Ni²⁺, K⁺, Ca²⁺, Ag⁺, Mg²⁺, Fe³⁺, Fe²⁺, Hg²⁺, Al³⁺, Cd²⁺, Pd²⁺, Co²⁺). Furthermore, the probe induced by Cu²⁺ and the π–π interaction of the aromatic unit can also form rod structure assembly, which can be observed by scanning electron microscopy (SEM).

© 2016 Elsevier Ltd. All rights reserved.

1. Introduction

The design and synthesis of efficient artificial receptors for various ions have received much interest in the last decade due to their essential roles in many places.^{1–10} Among these ions, copper(II) is the third most abundant transition-metal ion in the human body, and it plays an important role in many biological and environmental processes.⁵ Up to now, much effort has been made to detect copper(II) ions based on different analytical strategies,^{11–22} among which fluorometric methods have attracted considerable attention.

Benzo[1,2-b:4,5-b']dithiophene (BDT) unit has been the most popular donor for designing bulk heterojunction solar cells for its favor light harvesting and thermal stability.²³ In our previous work, BDT unit was formed copolymer with benzodithiophene and its photoelectric properties were studied.²⁴ Then we found that BDT unit has strong fluorescence. However, to the best of our knowledge, there are few researches for designing probe containing BDT as fluorophore.

At the same time, molecular self-assembly based on rational control of non-covalent interactions such as hydrophobic interactions, hydrogen bonding, aromatic stacking or metal coordination interactions, provides the design of self-assembly molecules from nanometer to micrometer scale.²⁵ Among these non-covalent interactions for molecular self-assembly, co-ordination compounds of metal ions with the organic ligands can result in interesting structures such as spherical particles,²⁶ rigid rods,²⁷ nanotubes²⁸ and springs²⁹ of micro to even nano dimension.

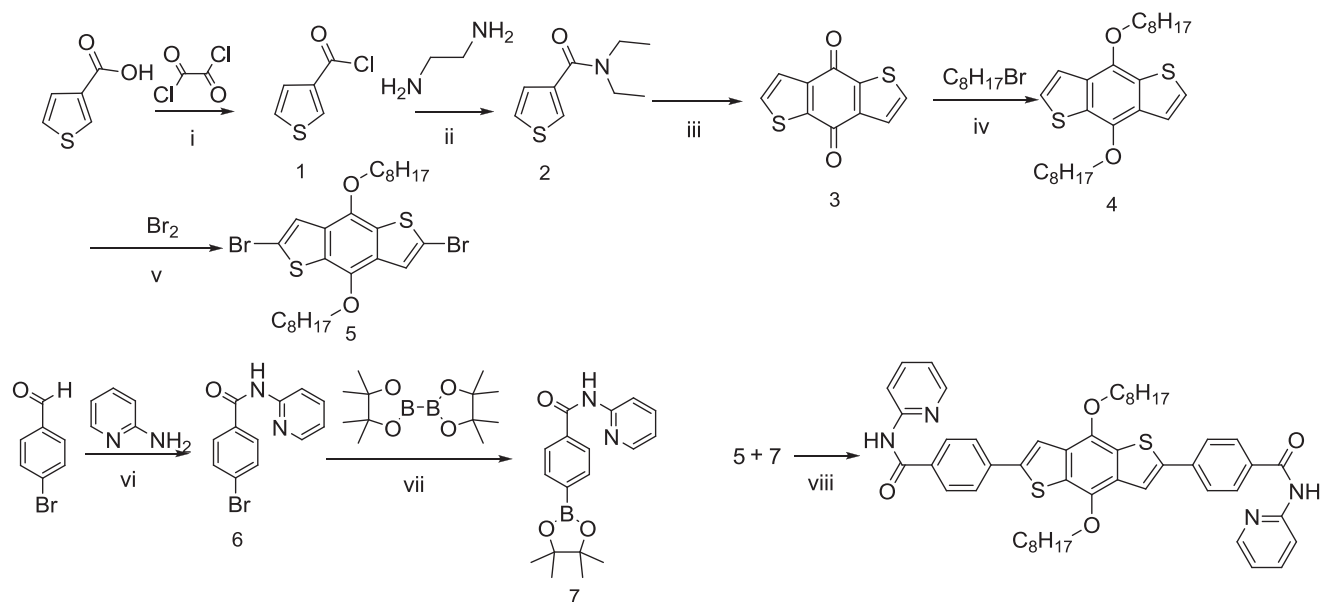
In this work, a novel probe was designed and synthesized, in which benzo[1,2-b:4,5-b']dithiophene (BDT) unit is used as fluorophore and two picolinamide units are used as metal-binding sites. To develop the probe of fluorophore–π conjugate spacer–receptor form, phenyl group is elongated the π-conjugation. Picolinamide unit has been utilized as a receptor and a suitable *p*-conjugated bridge. It is anticipated that the external metallic cations stimulus with picolinamide unit could modulate the intramolecular charge transfer, resulting in changes in the absorption spectra and fluorescence emission, thus the compound can be used as turn-off sensor for Cu²⁺ in a flash way, furthermore, transition metal Cu²⁺ can induce the compound to form metallosupramolecular assembly.

* Corresponding authors. Tel./fax: +86 21 64252967 (C.-Y.W.); e-mail addresses: jwzou@nit.net.cn (J. Zou), yjshen@ecust.edu.cn (Y. Shen), cwang@ecust.edu.cn (C. Wang).

2. Results and discussion

2.1. Synthesis

The synthesis route of BDT-BPBA was shown in Scheme 1. BDT-BPBA was synthesized by Suzuki coupling reaction of 4-bromo-*N*-(pyridin-2-yl)benzamide and *N*-(pyridin-2-yl)-4-(4,4,5,5-tetramethyl-1,3,2-dioxaborolan-2-yl)benzamide in 54% yield. The chemical structure of BDT-BPBA was confirmed by ^1H NMR, ^{13}C NMR and mass spectroscopic data (As shown in Fig. S1–S9).



(i) CH_2Cl_2 , r.t., overnight. (ii) CH_2Cl_2 , r.t., 30min, 84%. (iii) THF/*n*-BuLi, r.t., 30min, 71%. (iv) $\text{H}_2\text{O}/\text{Zn}/\text{NaOH}/\text{TBAB}$, reflu., 7h, 74%. (v) CH_2Cl_2 , r.t., 6h, 87%. (vi) DMF/CuI, 80°C, 24h, 63%. (vii) dioxane/KOAc/ Pd(dppf) Cl_2 , 100°C, overnight, 72%. (viii) toluene/ $\text{H}_2\text{O}/\text{K}_2\text{CO}_3$ / Pd(PPh $_3$) $_4$, reflu., 24h, 54%.

Scheme 1. The synthesis of BDT-BPBA.

2.2. Sensing response of BDT-BPBA for Cu^{2+}

The UV–vis spectra of BDT-BPBA with different amount of Cu^{2+} were investigated. As shown in Fig. 1, BDT-BPBA in DMSO/ H_2O (v:v=4:1) showed that two absorption peaks were centered at 358 nm and 422 nm. Upon additional of 0.5 equiv Cu^{2+} into the solution of BDT-BPBA, the two peaks were red-shift to 380 nm and 440 nm. The change of the UV–vis spectra can be explained by internal charge transfer (ICT) mechanism, which refers to the push–pull effect of the electron-donating and electron-withdrawing groups. That is, the red shift indicates that the energy gap of ICT band decreases, upon binding Cu^{2+} to the electron withdrawing moieties.³⁰

For fluorescence spectra (Fig. 2a), the emission wavelength of BDT-BPBA was appeared at 546 nm in DMSO/ H_2O (v:v=4:1) when excited by 410 nm photon. The fluorescence quantum yield can reach at 0.43. The fluorescence intensity was found to quench with the addition of Cu^{2+} . The quenching continues till addition of 0.5 equiv Cu^{2+} and remains constant thereafter. Under the common TLC-UV light, $\lambda=365$ nm, the yellow fluorescence quenching was observed by naked eyes when 0.5 equiv of Cu^{2+} was added to a 2×10^{-5} mol/L BDT-BPBA solution in DMSO/ H_2O (v:v=4:1) (Fig. 2b). The plot of F/F_0 as a function of Cu^{2+} concentration was shown in Fig. 3, where F_0 is the initial fluorescence intensity and F is

the fluorescence intensity at a particular concentration of Cu^{2+} , the ratio of the final fluorescence intensity to the initial fluorescence intensity was found to be 0.03.

From the titration experiment, it can be estimated that Cu^{2+} and picolinamide unit formed complex with a ratio of 1:2, and the ratio was confirmed by the Job's Plot (Fig. 4). The change in Job's Plot happened at $[\text{Cu}^{2+}]/([\text{Cu}^{2+}]+[\text{BDT-BPBA}])=0.33$, which meant that Cu^{2+} and BDT-BPBA formed a complex with a ratio of 1:2. It can be deduced that two picolinamide units of two BDT-BPBA molecules are in complex with one Cu^{2+} and two nitrogen atoms in each picoli-

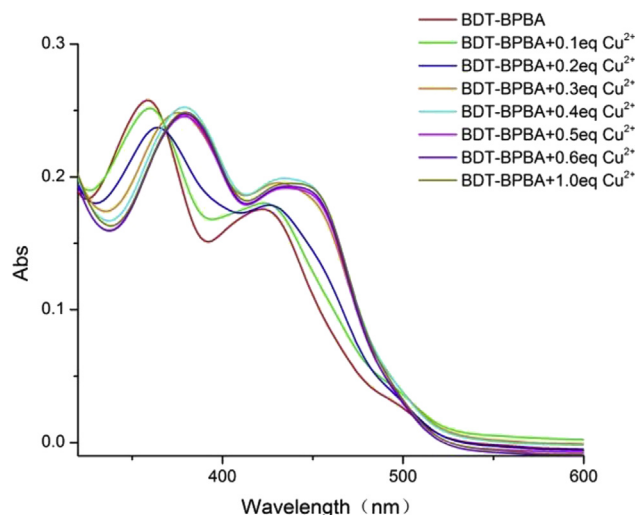


Fig. 1. UV–vis spectra of BDT-BPBA in DMSO/ H_2O (v:v=4:1) (2×10^{-5} mol/L) upon addition of 0.1–1.0 equiv of CuCl_2 .

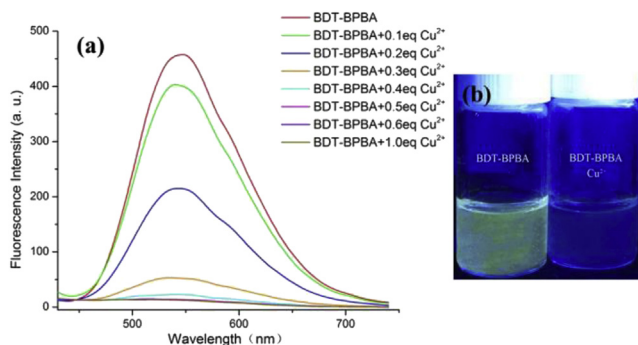


Fig. 2. (a) Fluorescence emission spectra of BDT-BPBA in DMSO/H₂O (v:v=4:1) (2×10^{-5} mol/L) upon addition of 0.1–1.0 equiv of CuCl₂ (b) Naked-eye fluorescent ($\lambda_{\text{ex}}=365$ nm) images of BDT-BPBA (2×10^{-5} mol/L) in DMSO/H₂O (v:v=4:1) solution upon the addition of 0.5 equiv of CuCl₂.

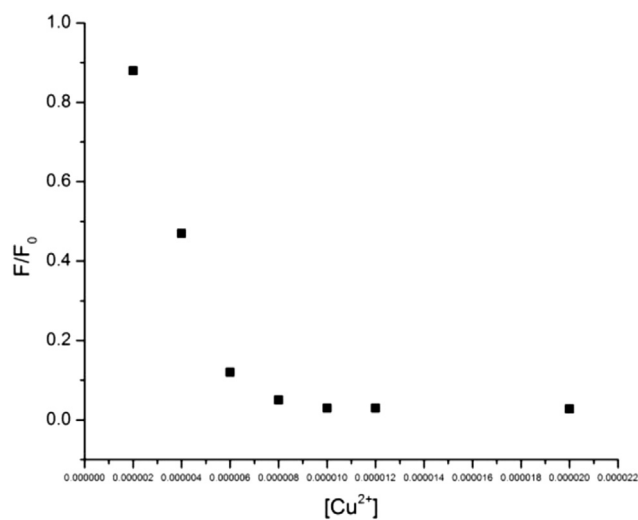


Fig. 3. The plot of F/F_0 for BDT-BPBA complex with Cu²⁺.

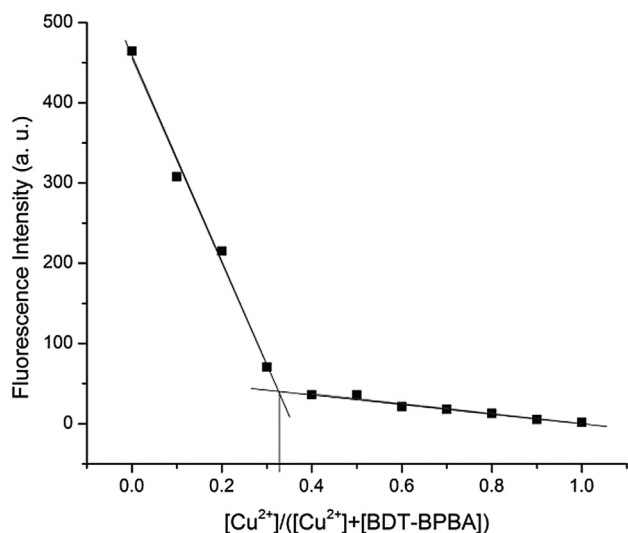


Fig. 4. Job's Plot for the complex of Cu²⁺ with BDT-BPBA determined by Fluorescence emission spectra.

namide unit coordinate with Cu²⁺ (Fig. 5). The detection limit can be calculated to be as low as 2.4×10^{-8} mol/L using $3\sigma/K$ (Fig. S10).

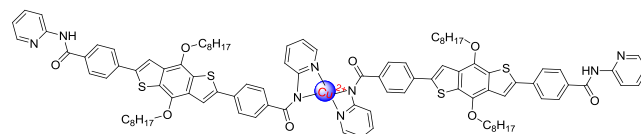


Fig. 5. The possible detection mechanism of Cu²⁺ by BDT-BPBA.

To further understand the fluorescence character of BDT-BPBA and the effect of metal ion titration, density functional theory (DFT) calculations at the B3LYP/LanI2dz level were performed for BDT-BPBA and its 2:1 complex with Cu²⁺, BDT-BPBA/Cu²⁺ (for the sake of simplicity, the OC₈H₁₇ group attached to the BDT unit was replaced by methoxy group in the actual calculations). The frontier molecular orbitals (HOMO and LUMO) of the BDT-BPBA monomer are shown in Fig. 6. As can be seen, both the HOMO (π) (−5.42 eV) and LUMO (π^*) (−2.18 eV) mainly reside at the BDT fragment, and the pyridine units have almost no distribution. The DFT calculation reveals that a lowest energy singlet transition of HOMO–LUMO characters with an energy gap of 3.24 eV. According to the fluorescence emission mechanism, the excited electron of BDT unit is back to the ground state and radiates strong fluorescence.

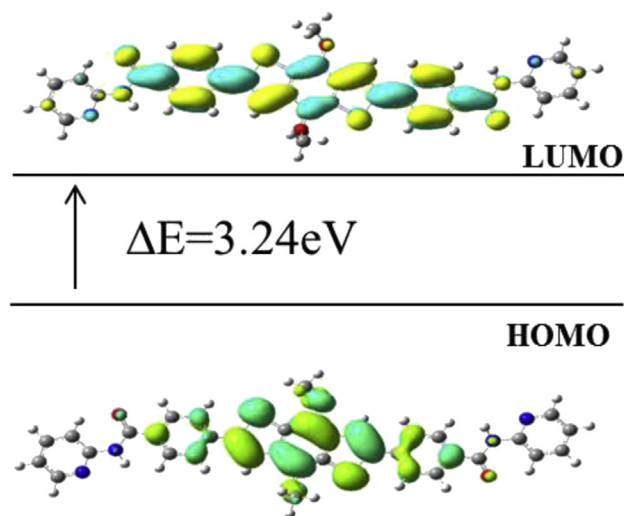


Fig. 6. DFT calculated molecular orbitals of BDT-BPBA.

For the 2:1 BDT-BPBA and Cu²⁺ coordination complex, geometrical optimizations show that four nitrogen atoms from two picolinamide units of BDT-BPBA ligands are coordinated with Cu²⁺ in the stable structure, while the carbonyl oxygen atoms do not participate in the coordination (Fig. 7a). Fig. 7b displays the contours of HOMO (π) (−5.55 eV) and LUMO (π^*) (−3.61 eV) of the complex BDT-BPBA/Cu²⁺. It can be seen that the HOMO and LUMO are located in two different BDT-BPBA ligands. As compared to the monomer, the HOMO energy level keeps almost unchanged, whereas the LUMO energy level is significantly lower. As a result, a lowest energy singlet transition of HOMO–LUMO characters the energy of 1.94 eV for BDT-BPBA/Cu²⁺. The decrease of energy gap can interpret that the two absorption peaks are red-shift after the addition of Cu²⁺. On the other hand, as the frontier molecular orbitals are spreading over two different ligands in the BDT-BPBA/Cu²⁺ complex, the excited electron of a BDT unit is back to the

ground state of another BDT unit, and therefore leads to the quenching of the fluorescence.

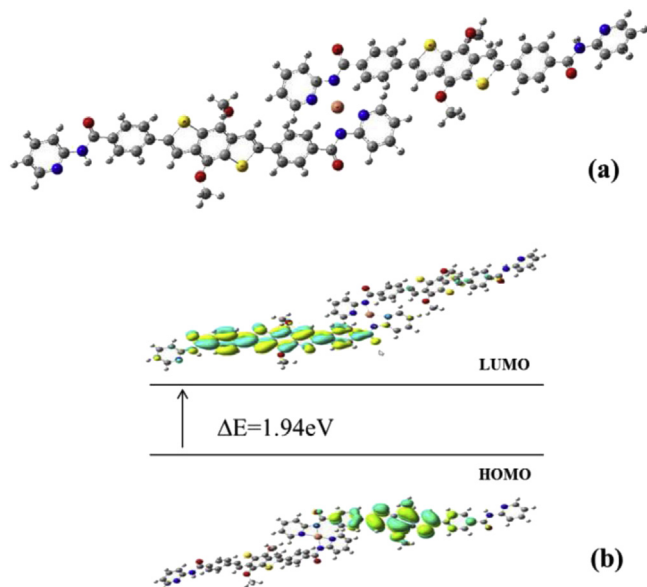


Fig. 7. (a) DFT optimized structure of BDT-BPBA/Cu²⁺ complex. (Ball color: Green=Cu, Blue=N, Red=O, Gray=C, White=H) (b) DFT calculated molecular orbitals of BDT-BPBA/Cu²⁺ complex.

2.3. Selective detection studies of Cu²⁺ by BDT-BPBA

The selectivity of BDT-BPBA towards a variety of metal ions (Mn²⁺, Pb²⁺, Cr³⁺, Zn²⁺, Ni²⁺, K⁺, Ca²⁺, Ag⁺, Mg²⁺, Fe³⁺, Fe²⁺, Hg²⁺, Al³⁺, Cd²⁺, Pd²⁺, Co²⁺) was examined through UV–vis spectra and fluorescence emission in DMSO/H₂O (v:v=4:1). As shown in Fig. 8, the absorption peaks were centered at 358 nm and 422 nm without further change when 0.5 equiv other ions were in presence. Upon the addition of 0.5 equiv Cu²⁺, these two peaks were red-shifted to 380 nm and 440 nm clearly, indicating the formation of the only species between BDT-BPBA and Cu²⁺. The results indicated that only Cu²⁺ could influence the electron transfer in BDT-BPBA molecule.

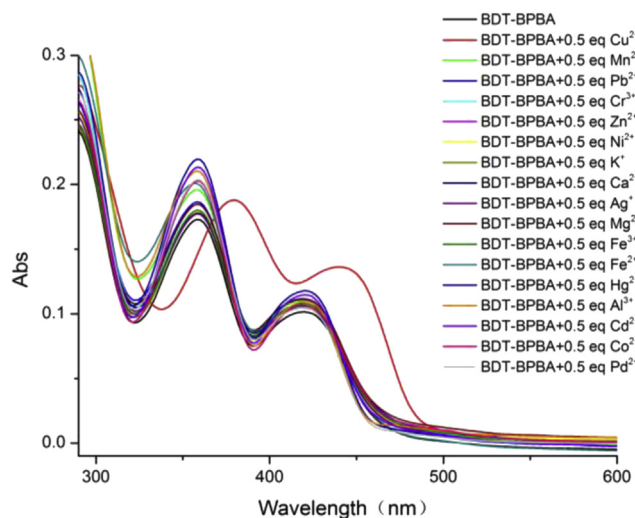


Fig. 8. UV–vis spectra of BDT-BPBA in DMSO/H₂O (v:v=4:1) (2×10^{-5} mol/L) upon addition of CuCl₂, MnCl₂, PbCl₂, CrCl₃, ZnCl₂, NiCl₂, KCl, CaCl₂, AgNO₃, MgCl₂, FeCl₃, FeCl₂, Hg(ClO₄)₂, AlCl₃, CdCl₂, PdCl₂, CoCl₂ (0.5 equiv).

In fluorescence spectra, BDT-BPBA alone has fluorescence emission at 546 nm with an excitation of 410 nm. When 0.5 equiv of various ions (Mn²⁺, Pb²⁺, Cr³⁺, Zn²⁺, Ni²⁺, K⁺, Ca²⁺, Ag⁺, Mg²⁺, Fe³⁺, Fe²⁺, Hg²⁺, Al³⁺, Cd²⁺, Pd²⁺, Co²⁺) were added to BDT-BPBA solution, respectively, it was found that the solution of BDT-BPBA exhibited no or small significant decrease of the fluorescence. The addition of 0.5 equiv Cu²⁺ resulted in drastic decrease of emission intensities at 546 nm (Fig. 9a). As shown in Fig. 9b, the fluorescence quenching could be observed only by additional of 0.5 equiv Cu²⁺, while the fluorescence not changed when other ions were exit under the TLC-UV light, $\lambda = 365 \text{ nm}$.

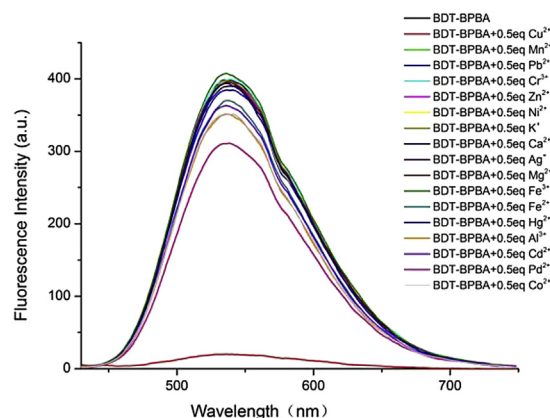


Fig. 9. (a) Fluorescence emission spectra of BDT-BPBA in DMSO/H₂O (v:v=4:1) (2×10^{-5} mol/L) upon addition of CuCl₂, MnCl₂, PbCl₂, CrCl₃, ZnCl₂, NiCl₂, KCl, CaCl₂, AgNO₃, MgCl₂, FeCl₃, FeCl₂, Hg(ClO₄)₂, AlCl₃, CdCl₂, PdCl₂, CoCl₂ (0.5 equiv) (b) Naked-eye fluorescent ($\lambda_{\text{ex}} = 365 \text{ nm}$) images of BDT-BPBA (2×10^{-5} mol/L) in DMSO/H₂O (v:v=4:1) solution upon the addition of CuCl₂, MnCl₂, PbCl₂, CrCl₃, ZnCl₂, NiCl₂, KCl, CaCl₂, AgNO₃, MgCl₂, FeCl₃, FeCl₂, Hg(ClO₄)₂, AlCl₃, CdCl₂, PdCl₂, CoCl₂ (0.5 equiv).

At the same time, the competition experiments were conducted in the presence of Cu²⁺ mixed with other relevant ions (Mn²⁺, Pb²⁺, Cr³⁺, Zn²⁺, Ni²⁺, K⁺, Ca²⁺, Ag⁺, Mg²⁺, Fe³⁺, Fe²⁺, Hg²⁺, Al³⁺, Cd²⁺, Pd²⁺, Co²⁺) (Fig. 10). When BDT-BPBA was treated with 0.5 equiv Cu²⁺ in the presence of 0.5 equiv other ions, the coexistent ions had

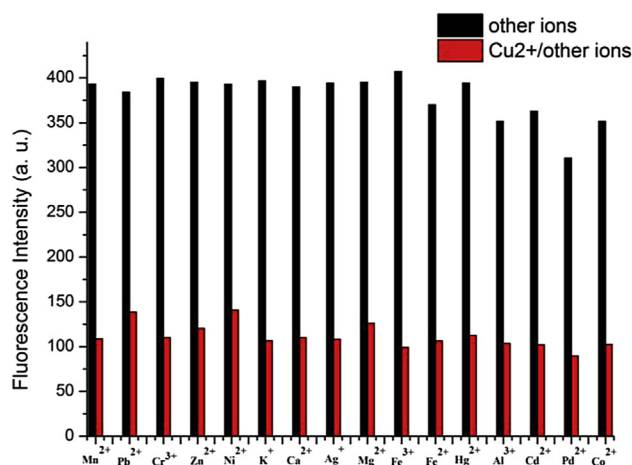


Fig. 10. The selectivity of BDT-BPBA in DMSO/H₂O (v:v=4:1) (2×10^{-5} mol/L) for Cu²⁺ in the presence of other metal ions (CuCl₂, MnCl₂, PbCl₂, CrCl₃, ZnCl₂, NiCl₂, KCl, CaCl₂, AgNO₃, MgCl₂, FeCl₃, FeCl₂, Hg(ClO₄)₂, AlCl₃, CdCl₂, PdCl₂, CoCl₂) (0.5 equiv).

a little effect on the emission intensity, Cu^{2+} can also influence the intermolecular electron transfer of BDT-BPBA and the fluorescence of the solution was reduced.

2.4. Self-assembly studies of BDT-BPBA/ Cu^{2+}

The assembly properties of BDT-BPBA/ Cu^{2+} was also studied by scanning electron microscopy (SEM) due to the characters of BDT-BPBA. Through the fluorescence titration and the theoretical calculations, it could be proved that picolinamide units of BDT-BPBA could form complex with Cu^{2+} and the binding constant between Cu^{2+} and picolinamides units is 3.93×10^3 L/mol according to UV–vis spectrum (Fig. S11). We inferred that Cu^{2+} may promote metal-assisted coordinative self-assembly of BDT-BPBA. As shown in Fig. 11, the molecules formed self-assembly in line with Cu^{2+} , furthermore, the BDT unit functionalized with phenyl-amide groups may also give directionality to the π stacked assembly of metal coordinated ligands.³¹ In order to confirm it, a tetrahydrofuran solution of the Cu^{2+} (0.1 mol/L, 0.1 mL) was dropped into the tetrahydrofuran solution of BDT-BPBA (0.01 mol/L, 2.0 mL). Then red precipitate was appeared gradually. A SEM image of the precipitate showed that many short rod structures are created (Fig. 12). The rod structure may be formed by the Cu^{2+} induced orientation and by the π – π interaction of the aromatic unit synchronously.

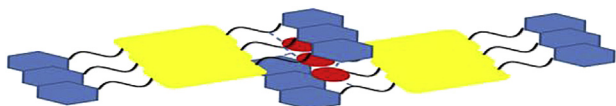


Fig. 11. Schematic representation of possible metal-directed self-assembly of BDT-BPBA.

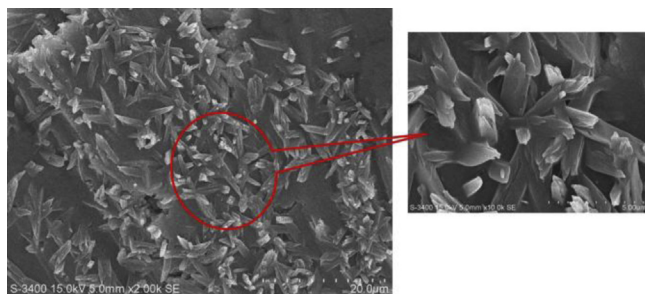


Fig. 12. SEM image of BDT-BPBA/ Cu^{2+} .

3. Conclusions

In summary, a new fluorescence probe BDT-BPBA containing benzo[1,2-*b*:4,5-*b'*]dithiophene (BDT) and two picolinamide units was synthesized through Suzuki coupling. To elongate the π conjugate spacer of the compound, phenyl was introduced. As a result, the fluorescence quantum yield of BDT-BPBA can achieve at 0.43. Through the titration test, the two absorption peaks centered at 358 nm and 422 nm red-shifted to 380 nm and 440 nm and the fluorescence intensity was almost quenched when addition of 0.5 equiv Cu^{2+} . The complex ratio is 1:2 between Cu^{2+} and BDT-BPBA, which was proved by Job's Plot and theoretical calculations. So, BDT-BPBA can be used as a turn-off probe for Cu^{2+} in a flash way and the detection limit is as low as 2.4×10^{-8} mol/L. It displayed well selectivity to Cu^{2+} over other ions (Mn^{2+} , Pb^{2+} , Cr^{3+} , Zn^{2+} , Ni^{2+} , K^+ , Ca^{2+} , Ag^+ , Mg^{2+} , Fe^{3+} , Fe^{2+} , Hg^{2+} , Al^{3+} , Cd^{2+} , Pd^{2+} , Co^{2+}) as well. On the other hand, it could form assembly in rod structure by the Cu^{2+} induced orientation, which can be confirmed by SEM.

4. Experimental section

4.1. Materials and measurements

All chemical reagents and solvents were purchased from commercial suppliers and were used without further purification unless otherwise note. Dioxane was dried with metal sodium and distilled immediately prior to use. All moisture-sensitive and air-sensitive reactions were carried out under argon atmosphere.

^1H NMR and ^{13}C NMR spectra were measured on a Bruker AM-400 spectrometer using *d*-chloroform or *d*₈-THF as a solvent and tetramethylsilane (TMS, $\delta=0$ ppm) as an internal standard. The UV–vis spectra were recorded on a Varian CARY 100 spectrophotometer at room temperature. Fluorescence-emission was detected on Varian Cary Eclipse spectrophotometer at room temperature. Scanning electron microscopy (SEM) was tested on Hitachi S-3400N SEM.

4.2. Synthetic procedures and characterizations

Compound 1–5 was synthesized similar to the literature.²³

4.2.1. Thiophene-3-carbonyl chloride (1). Thiophene-3-carboxylic acid (8.00 g, 62.43 mmol) were dissolved in 80 mL CH_2Cl_2 and cooled to 0 °C, then oxalyl chloride (12.0 mL, 140.87 mmol) was added into the reaction system. The reactant was stirred overnight at room temperature, and a light yellow solution was obtained. After removing the solvent, unreacted oxalyl chloride was removed under vacuum, yellow solid was obtained. It was dissolved into 20 mL of CH_2Cl_2 and used for the next step without further purified.

4.2.2. *N,N*-Diethylthiophene-3-carboxamide (2). Diethylamine (28.0 mL, 271.82 mmol) and 160 mL CH_2Cl_2 were mixed at 0 °C, and the solution of **1** was added into the reagent slowly. After all of the **1** solution was added, the reactant was stirred at room temperature for 30 min. Then, the reactant was washed by water (3×60 mL), and the organic layer was dried over Na_2SO_4 . After removing solvent, the crude product was purified by distillation under vacuum, and pale yellow oil was obtained in 84% yield. ^1H NMR (400 MHz, CDCl_3) δ (ppm): 7.47 (s, 1H), 7.33–7.31 (m, 1H), 7.18 (d, $J=4.0$ Hz, 1H), 3.51–3.29 (m, 4H), 1.23–1.17 (m, 6H).

4.2.3. 4,8-Dihydrobenzo[1,2-*b*:4,5-*b'*]dithiophen-4,8-dione (3). **2** (2.00 g, 10.9 mmol) was dissolved in 30 mL THF under argon atmosphere. The solution was cooled to 0 °C, and *n*-butyllithium (5.2 mL, 2.5 mol/L) was added dropwise within 30 min. Then, the reactant was stirred at room temperature for 30 min. The reactant was poured into 100 mL ice water and stirred for another 2 h. The mixture was filtrated, and the precipitate was washed by 10 mL water, 5 mL of methanol. **3** was obtained as yellow powder in 71% yield. Mp >200 °C ^1H NMR (400 MHz, CDCl_3), δ (ppm): 7.69 (d, $J=4.2$ Hz, 2H), 7.65 (d, $J=4.2$ Hz, 2H).

4.2.4. 4,8-Didodecyloxybenzo[1,2-*b*:3,4-*b'*]dithiophene (4). **3** (1.00 g, 4.5 mmol), zinc powder (0.71 g, 10.88 mmol), and 15 mL of water were mixed, then sodium hydroxide (2.73 g, 68.23 mmol) was added into the mixture. The mixture was well stirred and heated to reflux for 1 h. During the reaction, the color of the mixture changed from yellow to red and then to orange. Then, 1-bromododecane (2.4 mL, 13.67 mmol) and tetrabutylammonium bromide (293 mg, 0.91 mmol) were added. The color of the reactant should be yellow or orange. Then, the reactant was refluxed for 6 h. After completion of the reaction, the reactant was poured into water and extracted by CH_2Cl_2 (3×10 mL). The organic layer was dried over Na_2SO_4 . After removing solvent, the crude product was purified by silica column (eluent petroleum ether: $\text{CH}_2\text{Cl}_2=15:1$). White solid

was obtained in 74% yield. MP 46.0–47.1 °C ^1H NMR (400 MHz, CDCl_3) δ (ppm): 7.47 (d, $J=5.5$ Hz, 2H), 7.36 (d, $J=5.5$ Hz, 2H), 4.27 (t, $J=6.6$ Hz, 4H), 1.87 (q, $J=6.9$ Hz, 4H), 1.57–1.54 (m, 4H), 1.34–1.25 (m, 16H), 0.88 (t, $J=7.0$ Hz, 6H).

4.2.5. 2,6-Dibromo-4,8-didodecyloxybenzo[1,2-*b*;3,4-*b'*]dithiophene (5). **4** (1.37 g, 3.08 mmol) was dissolved into 30 mL of CH_2Cl_2 . Bromine (0.93 g, 6.15 mmol) was dissolved into 20 mL CH_2Cl_2 , slowly dropped into the reactant at 0 °C, and then the reactant was stirred for 6 h at room temperature. After the reaction was over, the solvent was removed under vacuum. The residue was purified by silica column (eluent petroleum ether: $\text{CH}_2\text{Cl}_2=10:1$) to get a white solid in 87% yield. Mp 58.9–59.3 °C ^1H NMR (400 MHz, CDCl_3) δ (ppm): 7.42 (s, 2H), 4.19 (t, $J=6.6$ Hz, 4H), 1.85–1.82 (m, 4H), 1.55–1.51 (m, 4H), 1.37–1.31 (m, 16H), 0.90 (t, $J=6.8$ Hz, 6H).

4.2.6. 4-Bromo-*N*-(pyridin-2-yl)benzamide (6).³² 4-Bromobenzaldehyde (200 mg, 1.09 mmol), pyridin-2-amine (153 mg, 1.63 mmol) and CuI (21 mg, 0.11 mmol) were dissolved in 5 mL DMF. The reaction mixture was stirred at 80 °C for 24 h. Then the reactant was extracted with CH_2Cl_2 (3×10 mL) and then washed by water (3×10 mL). The organic layer was dried by Na_2SO_4 . After removing the solvent, the crude product was purified by silica column (eluent petroleum ether: ethyl acetate=10:1) to get white solid in 63% yield. Mp 133.2–135.0 °C ^1H NMR (400 MHz, CDCl_3) δ (ppm): 8.64 (s, 1H) 8.37 (d, $J=8.4$ Hz, 1H) 8.30 (d, $J=5.9$ Hz, 1H) 7.81 (d, $J=8.6$ Hz, 2H) 7.77 (dd, $J_1=8.4$ Hz, $J_2=1.8$ Hz, 1H) 7.67–7.63 (m, 2H) 7.10–7.08 (m, 1H).

4.2.7. *N*-(Pyridin-2-yl)-4-(4,4,5,5-tetramethyl-1,3,2-dioxaborolan-2-yl)benzamide (7). **6** (200 mg, 0.72 mmol), bis(pinacolato)diboron (367 mg, 1.44 mmol) were combined in anhydrous dioxane. Potassium acetate (213 mg, 2.16 mmol) and Pd(dppf) Cl_2 (53 mg, 0.07 mmol) were added to the mixture under argon atmosphere. The mixture was stirred at 100 °C overnight. After evaporation of the solvent, the residue was purified by silica column (eluent petroleum ether: ethyl acetate=5:1) to get brown oil in 72% yield. ^1H NMR (400 MHz, CDCl_3) δ (ppm): 8.82 (s, 1H) 8.42 (d, $J=8.4$ Hz, 1H) 8.31 (d, $J=3.6$ Hz, 1H) 7.94 (s, 4H) 7.78 (t, $J=8.8$ Hz, 1H) 7.09 (dd, $J_1=6.6$ Hz, $J_2=5.0$ Hz, 1H) 1.37 (s, 12H).

4.2.8. 4,4'-(4,8-Didodecyloxybenzo[1,2-*b*;3,4-*b'*]dithiophene)bis(*N*-(pyridin-2-yl)benzamide) [BDT-BPBA]. **5** (133 mg, 0.21 mmol), **7** (207 mg, 0.64 mmol) and K_2CO_3 (236 mg, 1.68 mmol) were dissolved in toluene (20 mL) and water (5 mL). Then Pd(PPh $_3$) $_4$ (25 mg, 0.021 mmol) was added under Argon atmosphere. The reaction mixture was heated to reflux and stirred for 24 h. After completion of the reaction, CH_2Cl_2 (10 mL) and water (10 mL) were added into the reaction mixture. Then the organic layer was washed by water (10 mL \times 3) and dried over Na_2SO_4 . After the solvent was removed, the residue was purified by silica column (eluent petroleum ether: ethyl acetate=3:1) to get a yellow solid in 54% yield. Mp 199.4–201.9 °C ^1H NMR (400 MHz, CDCl_3) δ (ppm): 8.63 (s, 2H) 8.42 (d, $J=8.3$ Hz, 2H) 8.34 (d, $J=5.7$ Hz, 2H) 8.02 (d, $J=8.4$ Hz, 3H) 7.90–7.87 (m, 3H) 7.81–7.77 (m, 4H) 7.65 (s, 1H) 7.13–7.06 (m, 2H) 4.36 (t, $J=6.6$ Hz, 4H) 1.98–1.94 (m, 4H) 1.63–1.61 (m, 4H) 1.33–1.25 (m, 16H). ^{13}C NMR (100 MHz, d_8 -THF) δ (ppm): 164.81, 152.80, 147.80, 144.61, 142.55, 137.55, 137.17, 134.49, 132.85, 129.90, 128.49, 125.93, 119.14, 117.29, 114.02, 73.86, 31.88, 30.55, 29.66, 29.64, 29.34, 26.05, 22.60, 13.49. ESI-MS [$\text{M}+\text{H}^+$] calcd 839.3665, Found 839.3665.

4.3. UV–vis and fluorescence titration

BDT-BPBA (8.4 mg) was dissolved in 100 mL DMSO to get 1×10^{-4} mol/L solution. Then 1×10^{-4} mol/L solution was dilute to

2×10^{-5} mol/L solution (DMSO:H $_2$ O=4:1(v/v)). $\text{CuCl}_2 \cdot 2\text{H}_2\text{O}$ (17.0 mg) was dissolved in 10 mL deionized water to get 0.01 mol/L solution. 2.5 mL 2×10^{-5} mol/L BDT-BPBA solution was in cuvette, then 0.5 μL (0.1 equiv), 1.0 μL (0.2 equiv), 1.5 μL (0.3 equiv), 2.0 μL (0.4 equiv), 2.5 μL (0.5 equiv), 3.0 μL (0.6 equiv), and 5.0 μL (1.0 equiv) Cu^{2+} was added, respectively. After mixing them for a few seconds, UV–vis and fluorescence spectra were taken at room temperature.

4.4. UV–vis and fluorescence for selectivity

ZnCl_2 (0.0136 g), PbCl_2 (0.0278 g), FeCl_3 (0.0162 g), AgNO_3 (0.0170 g), $\text{NiCl}_2 \cdot 6\text{H}_2\text{O}$ (0.0238 g), CaCl_2 (0.0111 g), MgCl_2 (0.0095 g), KCl (0.0075 g), $\text{CrCl}_3 \cdot 6\text{H}_2\text{O}$ (0.0266 g), $\text{MnCl}_2 \cdot 4\text{H}_2\text{O}$ (0.0198 g), $\text{FeCl}_2 \cdot 4\text{H}_2\text{O}$ (0.0199 g), $\text{Hg}(\text{ClO}_4)_2 \cdot 3\text{H}_2\text{O}$ (0.0399 g) CdCl_2 (0.0183 g), $\text{CoCl}_2 \cdot 6\text{H}_2\text{O}$ (0.0238 g), AlCl_3 (0.0133 g), PdCl_2 (0.0177 g) were dissolved in 10 mL deionized water to get 0.01 mol/L solution, respectively. Then 2.5 μL (0.5 equiv) ion solution was added into 2.5 mL 2×10^{-5} mol/L BDT-BPBA solution. After mixing them for a few seconds, UV–vis and fluorescence spectra were taken at room temperature.

4.5. Job's plot measurements

500 μL , 450 μL , 400 μL , 350 μL , 300 μL , 250 μL , 200 μL , 150 μL , 100 μL , 50 μL and 0 μL 1×10^{-4} mol/L BDT-BPBA solution were taken and transferred to cuvette. 0 μL , 0.5 μL , 1.0 μL , 1.5 μL , 2.0 μL , 2.5 μL , 3 μL , 3.5 μL , 4.0 μL , 4.5 μL and 5.0 μL 0.01 mol/L CuCl_2 solution was added into each cuvette, and 0.5 mL deionized water was added into each cuvette. Then each cuvette was dilute to 2.5 mL. After mix a few seconds, fluorescence spectra were taken at room temperature.

4.6. Calculation of detection limit

The detection limit was determined from the fluorescence titration data based on $3\sigma/K$. Ten times of fluorescence intensity of BDT-BPBA were tested and σ can be calculated. According to the result of fluorescence titrating experiment, the fluorescent intensity data of BDT-BPBA were normalized between the minimum intensity and the maximum intensity, respectively when excited by 410 nm. The linear regression curve was then fitted to these normalized fluorescent intensity data, and the slop K of line could be calculated.

Acknowledgements

The authors are grateful to financial support from the National Natural Science Foundation of China (Nos. 20872035, 21576087), Key Laboratory of Organosilicon Chemistry and Material Technology of Ministry of Education, Hangzhou Normal University, and the East China University of Science and Technology.

Supplementary data

Supplementary data (^1H NMR, ^{13}C NMR, and MS of BDT-BPBA are available. Additional graph for calculation of detection limit and binding constant can be found in ESI) associated with this article can be found in the online version, at <http://dx.doi.org/10.1016/j.tet.2016.03.029>.

References and notes

- Amendola, V.; Fabbri, L.; Mosca, L. *Chem. Soc. Rev.* **2010**, *39*, 3889–3915.
- Li, A. F.; Wang, J. H.; Wang, F.; Jiang, Y. B. *Chem. Soc. Rev.* **2010**, *39*, 3729–3745.
- Basu, A.; Dey, S. K.; Das, G. *RSC Adv.* **2013**, *3*, 6596–6605.

4. Chen, B.; Song, F. L.; Fan, J. L.; Peng, X. J. *Chem.—Eur. J.* **2013**, *19*, 10115–10118.
5. Que, E. L.; Domaille, D. W.; Chang, C. J. *Chem. Rev.* **2008**, *108*, 1517–1549.
6. Zhang, J. Q.; Zhai, C. X.; Wang, F.; Zhang, C. J.; Li, S. J.; Zhang, M. M.; Li, N.; Huang, F. H. *Tetrahedron Lett.* **2008**, *49*, 5009–5012.
7. Zhu, K. L.; Li, S. J.; Wang, F.; Huang, F. H. *J. Org. Chem.* **2009**, *74*, 1322–1328.
8. Yu, G. C.; Zhang, Z. B.; Han, C. Y.; Xue, M.; Zhou, Q. Z.; Huang, F. H. *Chem. Commun.* **2012**, 2958–2960.
9. Ji, X. F.; Yao, Y.; Li, J. Y.; Yan, X. Z.; Huang, F. H. *J. Am. Chem. Soc.* **2013**, *135*, 74–77.
10. Wang, P.; Yao, Y.; Xue, M. *Chem. Commun.* **2014**, 5064–5067.
11. Zou, Q.; Li, X.; Zhang, J.; Zhou, J.; Sun, B.; Tian, H. *Chem. Commun.* **2012**, 2095–2097.
12. He, J. J.; He, J. X.; Wang, T. T.; Zeng, H. P. *J. Mater. Chem. C* **2014**, *2*, 7531–7540.
13. Liu, W. Y.; Li, H. Y.; Zhao, B. X.; Miao, J. Y. *Analyst* **2012**, *137*, 3466–3469.
14. Basa, P. N.; Sykes, A. G. *J. Org. Chem.* **2012**, *77*, 8428–8434.
15. Lee, S. A.; Lee, J. J.; Shin, J. W.; Min, K. S.; Kim, C. *Dyes Pigm.* **2015**, *116*, 131–138.
16. Yu, M. M.; Yuan, R. L.; Shi, C. X.; Zhou, W. L.; Wei, H.; Li, Z. X. *Dyes Pigm.* **2013**, *99*, 887–894.
17. Lin, Q.; Chen, P.; Liu, J.; Fu, Y. P.; Zhang, Y. M.; Wei, T. B. *Dyes Pigm.* **2013**, *98*, 100–105.
18. Liu, Z. P.; Zhang, C. L.; Wang, X. Q.; He, W. J.; Guo, Z. J. *Org. Lett.* **2012**, *14*, 4378–4381.
19. Li, P.; Duan, X.; Chen, Z. Z.; Liu, Y.; Xie, T.; Fang, L.; Li, X.; Yin, M.; Tang, B. *Chem. Commun.* **2011**, 7755–7757.
20. Xia, S.; Liu, G.; Pu, S. J. *Mater. Chem. C* **2015**, *3*, 4023–4029.
21. Ma, Y. W.; Lai, G. Q.; Li, Z. F.; Wang, C. Y.; Shen, Y. J. *Tetrahedron* **2015**, *71*, 8717–8724.
22. Wang, P.; Xing, H.; Xia, D. Y.; Ji, X. F. *Chem. Commun.* **2015**, 17431–17434.
23. Hou, J. H.; Park, M. H.; Zhang, S. Q.; Yao, Y.; Chen, L. M.; Li, J. H.; Yang, Y. *Macromolecules* **2008**, *41*, 6012–6018.
24. Jiang, S. Y.; Ma, Y. W.; Wang, Y. Y.; Wang, C. Y.; Shen, Y. J. *Chin. J. Chem.* **2014**, *32*, 298–306.
25. Babu, S. S.; Kartha, K. K.; Ajayaghosh, A. *J. Phys. Chem. Lett.* **2010**, *1*, 3413–3424.
26. Sun, X.; Dong, S.; Wang, E. *J. Am. Chem. Soc.* **2005**, *127*, 13102–13103.
27. Feng, H. T.; Song, S.; Chen, Y. C.; Shen, C. H.; Zheng, Y. S. *J. Mater. Chem. C* **2014**, *2*, 2353–2359.
28. Liu, B.; Qian, D. J.; Chen, M.; Wakayama, T.; Nakamura, C.; Miyake, J. *Chem. Commun.* **2006**, 3175–3177.
29. Kim, H. J.; Lee, E.; Park, H. S.; Lee, M. J. *J. Am. Chem. Soc.* **2007**, *129*, 10994–10995.
30. Park, G. J.; Hwang, I. H.; Song, E. J.; Kim, H.; Kim, C. *Tetrahedron* **2014**, *70*, 2822–2828.
31. Jain, A.; Rao, K. V.; Goswami, A.; George, S. J. *J. Chem. Sci.* **2011**, *123*, 773–781.
32. Yang, S. Z.; Yan, H.; Ren, X. Y.; Shi, X. K.; Li, J.; Wang, Y. L.; Huang, G. S. *Tetrahedron* **2013**, *69*, 6431–6435.